Probing the mass effect of heavy quark jets in high-energy nuclear collisions*

Sa Wang (王洒)[1,2,3] Shuang Li (李双)[1,2] Yao Li (李瑶)[3] Ben-Wei Zhang (张本威)[3†] Enke Wang (王恩科)[4]

[1]College of Science, China Three Gorges University, Yichang 443002, China
[2]Center for Astronomy and Space Sciences and Institute of Modern Physics, China Three Gorges University, Yichang 443002, China
[3]Key Laboratory of Quark & Lepton Physics (MOE) and Institute of Particle Physics, Central China Normal University, Wuhan 430079, China
[4]Guangdong-Hong Kong Joint Laboratory of Quantum Matter, Guangdong Provincial Key Laboratory of Nuclear Science, Southern Nuclear Science Computing Center, South China Normal University, Guangzhou 510006, China

Abstract: The production of heavy-quark (HQ) jets is a new area that addresses the mass effect of jet quenching in heavy-ion physics. This paper presents a theoretical study of HQ jet yield suppression in Pb+Pb collisions at the Large Hadron Collider (LHC) and focuses on the energy loss of HQ jets produced by different mechanisms. The p+p baseline is provided by the generator simulation of high-energy reactions of particles (SHERPA), and the jet-medium interactions are described by the SHELL transport model, which considers the elastic and inelastic partonic energy loss in the quark-gluon plasma (QGP). In p+p collisions, our numerical results indicate that the HQ jets from gluon splitting ($g \to Q$-jet) are the dominant contribution at high p_T, displaying more dispersive structures than the HQ-initiated ($Q \to Q$-jet). In nucleus-nucleus collisions, our calculations were consistent with the inclusive and b-jet R_{AA} recently measured by the ATLAS collaboration, revealing a remarkable manifestation of the mass effect of jet energy loss. As a result of the dispersive substructure, the $g \to Q$-jet loses more energy than the $Q \to Q$-jet in the QGP. Due to the significant contribution of $g \to c$-jet, the R_{AA} of c-jet is comparable or even smaller than that of inclusive jet. To experimentally distinguish the $g \to Q$-jet and $Q \to Q$-jet, we propose event selection strategies based on their topological features and test their performances. By isolating the $c \to c$-jet, $b \to b$-jet, and the jets initiated by heavy quarks, we predicted that the order of their R_{AA} are in line with the mass hierarchy of energy loss. Future measurements on the R_{AA} of $Q \to Q$-jet and $g \to Q$-jet will provide a unique opportunity for testing the flavor/mass dependence of energy loss at the jet level.

Keywords: heavy-ion collisions, quark-gluon plasma, jet quenching, heavy quark jet, energy loss

DOI: 10.1088/1674-1137/adb385 **CSTR:** 32044.14.ChinesePhysicsC.49064101

I. INTRODUCTION

High-energy nuclear collisions at the Relativistic Heavy Ion Collider (RHIC) and Large Hadron Collider (LHC) provide an excellent opportunity for unraveling the mysteries of the quark-gluon plasma (QGP), a new state of nuclear matter formed at extremely high temperatures and densities. The "jet quenching" effect, referring to the energy attenuation of fast partons due to their strong interactions with the constituents of the QGP medium, has piqued the interest of physicists who have studied them extensively [1−21]. Investigations of the jet quenching phenomenon have deepened our understanding of the quantum chromodynamics (QCD) under extreme conditions and revealed the properties of the strongly-coupled nuclear matter [22−24].

As a result of the large mass ($M_Q \gg \Lambda_{\rm QCD}$), heavy quarks (HQ) are powerful hard probes for exploring the transport properties of the QGP [25−30]. Over the past two decades, measurements on the nuclear modification factor R_{AA} [31−34] and collective flow v_n [35−38] of heavy-flavor hadrons have enriched our knowledge with regard to the energy loss mechanisms and hadronization patterns of heavy quarks in high-energy heavy-ion collisions. Because of the "dead-cone" effect [39], heavy quarks lose less energy than the massless light partons [40−42]. By comparing the R_{AA} of heavy-flavor hadrons [43−46] and their decayed leptons [47−49] with those of light-flavor ones, evidence of the mass effect has been partly addressed [50−52].

The HQ jets, defined as jets containing heavy-flavor quarks/hadrons [53, 54], are also excellent tools for cap-

Received 13 November 2024; Accepted 6 February 2025; Published online 7 February 2025

* Supported by the MajorProject of Basic and Applied Basic Research of Guangdong Province, China (2020B0301030008, 2023A1515011460), and the National Natural Science Foundation of China (11935007, 12035007, 12247127, 12375137). Sa Wang is supported by the Open Foundation of Key Laboratory of Quark and Lepton Physics (MOE) (QLPL2023P01) and the Talent Scientific Star-up Foundation of the China Three Gorges University, China (CTGU) (2024RCKJ013)

† E-mail: bwzhang@mail.ccnu.edu.cn

turing the mass effect of energy loss at the jet level [55−63]. The richer inner structure of HQ jets compared to that of single particles provides a unique opportunity for exploring the exquisite interaction mechanisms between the hard parton and the medium. The investigation of the production mechanisms and substructures of HQ jets has also attracted much attention both experimentally [64−71] and theoretically [72−81]. The recent measurements on the jet radial profile [64] and jet shape by the Compact Muon Solenoid (CMS) collaboration [69] imply that the HQ jets produced by different mechanisms may exhibit distinct topologies and structures [82, 83]. In this context, it would be of great interest to explore the energy loss effect of HQ jets produced by different channels and their relation to their substructures. Note that the HQ jet samples selected in the experiment included the jets initiated by heavy quarks ($Q \to Q$-jet) and a considerable contribution from the gluon splitting ($g \to Q$-jet). The former is initiated by a heavy quark created in the early stages of the QCD hard scattering, whereas the latter can be produced by the splitting of a high-energy gluon ($g \to Q\bar{Q}$) during the parton shower. However, experimentally comparing the mass effect of the jet energy loss of the HQ-initiated jet with that of the massless one is challenging. Suitable selection strategies can be explored to isolate the HQ jets produced by different production mechanisms, to enable a direct comparison of the yield suppression of the HQ-initiated jets with that of the light-flavor ones.

In this study, the yield suppression of HQ jets in heavy-ion collisions was explored to address the mass effect of jet energy loss. At first, the fractional contributions from different production mechanisms to the HQ jet yields in p+p collisions was estimated, further discussing their main characteristics in the jet substructure. In nucleus-nucleus collisions, we systematically estimated the fractional contribution and energy loss of HQ jets from $Q \to Q$-jet and $g \to Q$-jet, demonstrating that a significant contribution of $g \to Q$-jet and its dispersive jet substructure \lead to a comparable R_{AA} of the c-jet relative to the inclusive jet. Furthermore, to realize the separation of $g \to Q$-jet and $Q \to Q$-jet in experimental measurements, strategies are proposed to distinguish them based on their topological features. By comparing the yield suppression of the select $Q \to Q$-jet sample with that of the inclusive jet, we show that the mass hierarchy of energy loss ($\Delta E_{\rm incl-jet} > \Delta E_{\rm c-jet} > \Delta E_{\rm b-jet}$) at the jet level holds true.

The remainder of this paper is organized as follows. In Sec. II, the mechanisms of producing HQ jets in p+p collisions is presented. In Sec. III, the theoretical framework of the transport model used to study the medium modifications of the HQ jet is introduced. In Sec. IV, the main results and specific discussions are provided. Finally, the work is summarized in Sec. IV.

II. HEAVY QUARK JET PRODUCTION IN *P+P* COLLISIONS

Production of open heavy flavors in hadron collisions has been studied over the past decades using various theoretical schemes [84−89]. Fig. 1 displays the typical QCD Feynman diagrams contributing to the production of HQ jets, which are usually categorized into three classes: flavor creation (FCR), flavor excitation (FEX), and gluon splitting (GSP) [82, 83]. The first two represent the pair creation of heavy quarks in hard scattering at leading order, in which the incoming partons are light quarks or gluons, and the outcoming $Q\bar{Q}$ pairs usually emerge back-to-back in azimuth. Higher-order QCD processes of heavy quark production are not negligible in hadron collisions at the LHC energy. Diagrams 1(c) and 1(d) represent the FCR processes at next-to-leading order (NLO) with an extra radiated gluon in the final state. Fig. 1(e) depicts the typical FEX process, in which a heavy quark from the parton distribution function of one incoming proton is excited in hard scattering by a light parton of another proton. The most distinct feature of FEX compared to FCR is that only one heavy quark is produced by the hard scattering. The last diagram in Fig. 1 depicts the splitting process of a final-state hard gluon during the parton shower, whereby in general, $Q\bar{Q}$ pairs are produced with a smaller opening angle in azimuth compared to that of FCR. The prior clarification of the different kinematics features of these subprocesses may help us understand the corresponding substructures and topological features of HQ jets.

In this study, we employed the Monte Carlo event generator simulation of high-energy reactions of particles

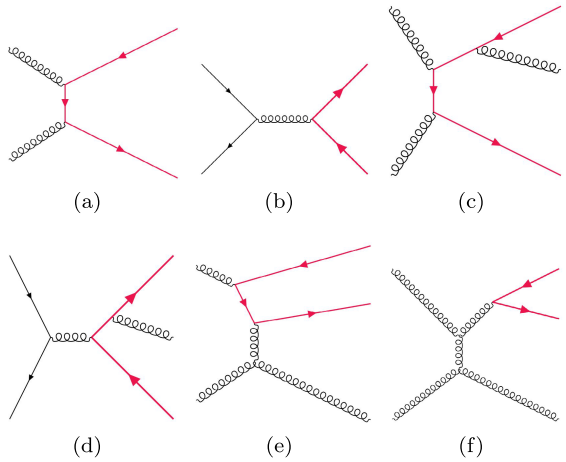

Fig. 1. (color online) Typical examples of QCD Feynman diagrams contributing to the production of HQ jets. Flavor creation: (a, b) LO; (c, d) NLO; (e) Flavor excitation; (f) Gluon splitting. Red fermion lines denote the produced heavy quarks.

(SHERPA) [90, 91] to compute the initial HQ jet production in p+p collisions, which matches that of the hard QCD processes at next-to-leading order with the vacuum parton shower effect (NLO+PS). The resummation of the parton shower based on Catani-Seymour subtraction method [92] is merged with fixed-order NLO calculations based on the MC@NLO prescription [93]. The NNPDF 3.0 [94] parton distribution functions (PDFs) were chosen for the SHERPA calculations. In the upper panel of Fig. 2, the calculated differential cross section of the D^0 meson tagged-jet by SHERPA in p+p collisions at $\sqrt{s}$ = 5.02 TeV are compared with a large ion collider experiment (ALICE) data [95]. The charged jets are reconstructed by using the Fastjet program [96] with anti-k_T algorithm [97] at R = 0.2, 0.4, 0.6 and rapidity range $|\eta^{\rm jet}| < 0.9 - R$. The D^0 mesons are required to have $2 < p_T^D < 36$ GeV. In the lower panel of Fig. 2, the yield of b-jet in p+p collisions at $\sqrt{s} = 5.02$ TeV compared with a toroidal LHC apparatus (ATLAS) and ALICE data [59, 98]. For the ATLAS measurement, the b-jets were constructed using the anti-k_T jet algorithm for $R = 0.2$ and $R = 0.4$ within $|y_{\rm jet}| < 2.1$. As for the ALICE data, the b-jet were constructed using charged particles with $R = 0.4$ within $|\eta_{\rm jet}| < 0.5$. The calculations by SHERPA are consistent with the experimental measurements of the HQ jet yields both for c-jet and b-jet, establishing a good baseline for subsequent studies of nuclear modifications.

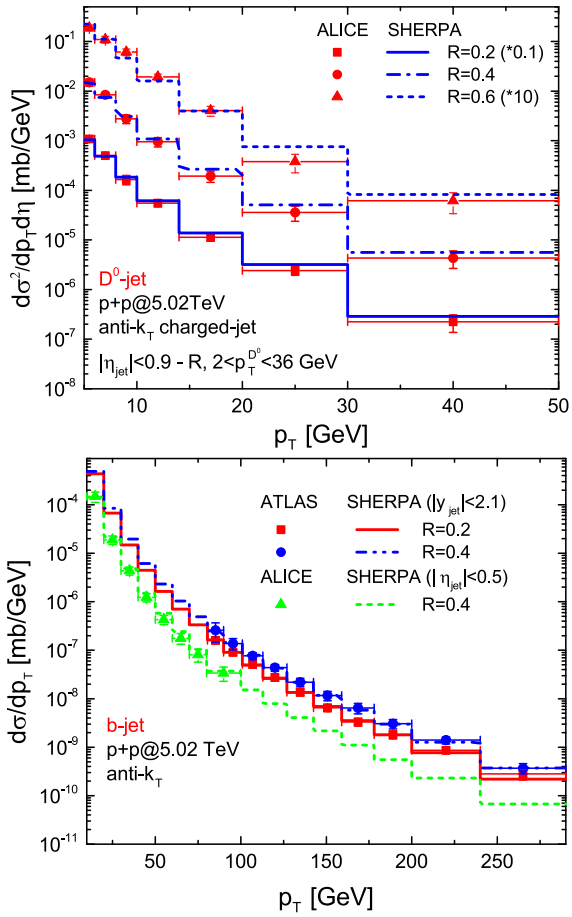

Fig. 2. (color online) Upper panel: differential cross sections of the D^0 meson tagged-jet by SHERPA in p+p collisions at $\sqrt{s}$ = 5.02 TeV compared with the ALICE data [95], at R = 0.2, 0.4, 0.6. Lower panel: differential cross section of b-jet in p+p collisions at $\sqrt{s}$ = 5.02 TeV compared with ALICE [98] and ATLAS [59] data.

In Monte Carlo simulations, the three mechanisms mentioned in Fig. 1 can be distinguished based on their topological features. The events that produce one and two heavy quarks in the hard processes can be categorized into FEX and FCR, respectively. In contrast, the events for the HQ jet created only in the parton shower stage are regarded as the GSP type. As shown in Fig. 3, the fractional contributions of the three mechanisms to the total yield was estimated as a function of jet p_T for both c-jet (upper) and b-jet (lower) in p+p collisions at $\sqrt{s}$ = 5.02 TeV. At $12 < p_T < 400$ GeV, The proportions of GSP increase with jet p_T and eventually become the most dominant mechanism for both c-jet and b-jet production, which is consistent with the estimation in [83]. For c-jet, at lower p_T the contributions of these three mechanisms are nonnegligible. As for b-jet, at lower p_T, the most important contributioons (above 50%) are from the FEX mechanism, in contrast to the GSP contributing less than 20%. FCR and FEX denote the jets initiated by heavy quarks, whereas GSP corresponds to HQ jets initiated by high-energy gluon. Focusing on their essential differences makes it convenient to categorize these three mechanisms into two subprocesses, $Q \to Q$-jet and $g \to Q$-jet, in the remainder of this paper.

To inuitibely show the essential differences of $Q \to Q$-jet and $g \to Q$-jet in substructures, two-dimensional (z_Q, r_Q) diagrams of these two types of jets are plotted in Figs. 4 and 5 in p+p collisions at $\sqrt{s}$ = 5.02 TeV for both c-jet and b-jet. Here $z_Q = p_T^Q / p_T^{\rm jet}$ denotes the transverse momentum fraction carried by heavy quarks in jets, and $r_Q = \sqrt{(\phi_Q - \phi_{\rm jet})^2 + (\eta_Q - \eta_{\rm jet})^2}$ is the radial distance of heavy quarks to the jet axis. The two observables, z_Q and r_Q, quantify the energy dominance of heavy quarks in jets and their angular location in the jet cone. For $Q \to Q$-jet of both c-jet and b-jet, the most heavy quarks carry above 80% of the jet momentum; and their moving directions collimate with the jet axis. Understandably, heavy quarks still dominate the jet's momentum even after soft shower evolution. However, the situation is quite different for the $g \to Q$-jet in the lower panels, where heavy quarks are more dispersed in the (z_Q, r_Q) diagrams. We observe a banded region, especially for the $g \to c$-jet, which is distinctly different from that of $c \to c$-jet. Plenty of heavy quarks produced by the gluon splitting carry smaller energy fractions and are loc-

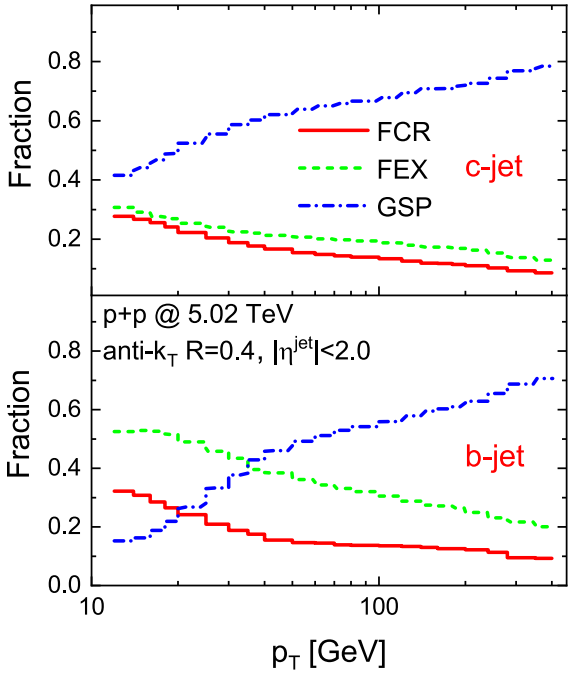

Fig. 3. (color online) The fractional contributions of the three production mechanisms to the total HQ jet differential cross section as functions of jet p_T in p+p collisions at $\sqrt{s}$ = 5.02 TeV for c-jet and b-jet.

ated in larger radii in jets. In the remainder of this paper, we show that the large fraction of $g \to Q$-jet and its distinct substructure compared to $Q \to Q$-jet play critical roles in the energy loss and yield suppression of HQ jets in high-energy nucleus-nucleus collisions.

III. JET TRANSPORT IN THE QUARK-GLUON PLASMA

Because of the large mass ($M_Q \gg T$), the heavy quarks are effective hard probes for the properties of the hot and dense QCD matter formed in high-energy nuclear collisions. In this study, we utilized the p+p events produced by SHERPA as input of the transport model driven by the modified Langevin equations [99−104] to estimate the nuclear modification effect of the HQ jet production in A+A collisions.

$$\mathrm{d}x_j = \frac{p_j}{E}\mathrm{d}t, \tag{1}$$

$$\mathrm{d}p_j = -\Gamma p_j \mathrm{d}t + \sqrt{\mathrm{d}t}C_{jk}(|\boldsymbol{p}+\xi \mathrm{d}\boldsymbol{p}|)\rho_k - p_j^{\mathrm{g}}. \tag{2}$$

The spatial position update of the traversing heavy

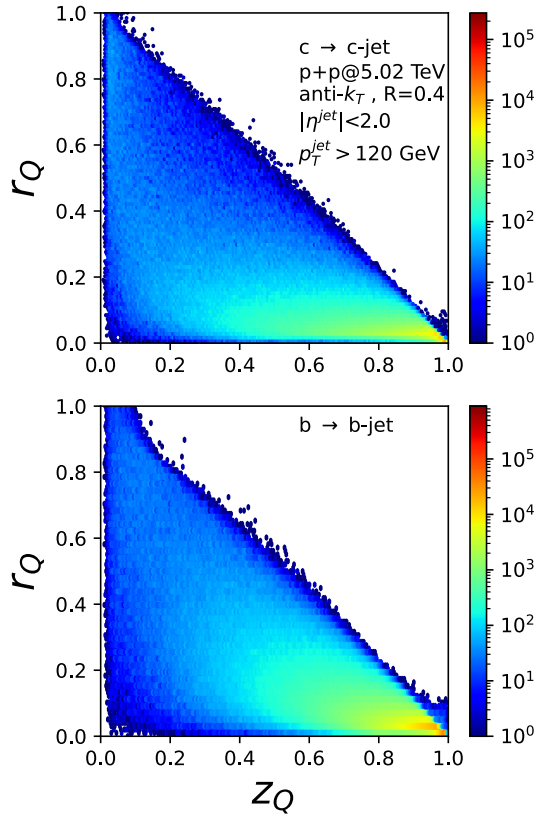

Fig. 4. (color online) Two-dimensional (z_Q, r_Q) correlation diagrams of $c \to c$-jet (upper panel) and $b \to b$-jet (lower panel) in p+p collisions at $\sqrt{s}$ = 5.02 TeV.

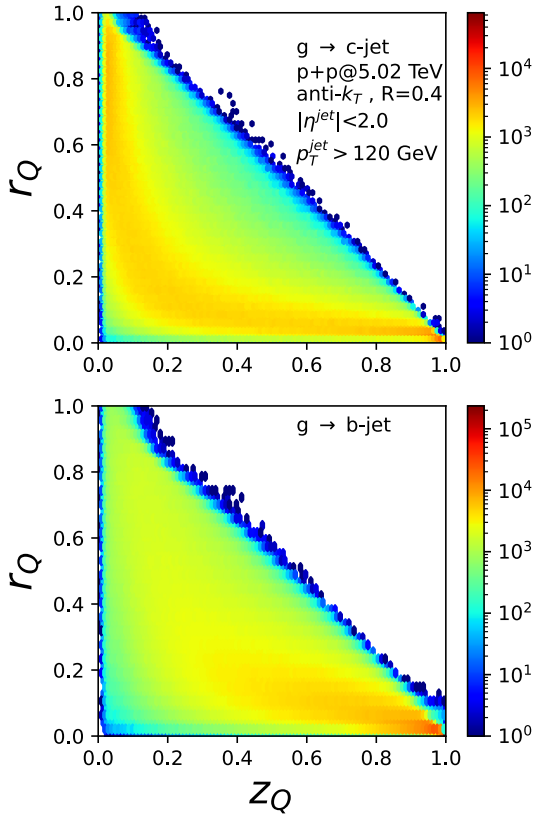

Fig. 5. (color online) Two-dimensional (z_Q, r_Q) correlation diagrams of $g \to c$-jet (upper panel) and $g \to b$-jet (lower panel) in p+p collisions at $\sqrt{s}$ = 5.02 TeV.

quarks in the medium is described in Eq. (1), where $\mathrm{d}t = 0.1$, and fm is the time step of our simulation. Meanwhile, Eq. (2) expresses the in-medium energy loss with index $j,k = 1,2,3$, where the three terms on the right-hand side denote the drag, thermal stochastic, and radiative correction terms, respectively. The drag term represents the collisional energy loss of heavy quarks, with the drag coefficient Γ controlling the strength of the energy loss. The thermal stochastic term indicates the mass of random kicks that heavy quarks suffer, caused by the thermal quasi-particles in the hot and dense QCD matter, where the white ρ_k obeys the standard normal distribution, and $P(\rho) = (2\pi)^{-3/2}\mathrm{e}^{\rho^2/2}$. The momentum argument of the covariance matrix C_{jk} is a function of the momentum diffusion coefficients in the longitudinal ($\kappa_\parallel$) and transverse ($\kappa_\perp$) directions [105].

$$C_{jk} = \sqrt{\kappa_\parallel}\frac{p_j p_k}{\vec{p}^2} + \sqrt{\kappa_\perp}\left(\delta_{jk} - \frac{p_j p_k}{\vec{p}^2}\right). \tag{3}$$

Note here we chose $\xi = 0$ for the pre-point (Ito) realization of the stochastic integral of $C_{jk}(|\boldsymbol{p} + \xi \mathrm{d}\boldsymbol{p}|)$ [106]. Additionally, by assuming κ is isotropic for heavy quarks $\kappa_\perp = \kappa_\parallel = \kappa$, a simple expression $C_{jk} = \sqrt{\kappa}\delta_{jk}$ can be obtained. Then the momentum diffusion coefficient κ can be related to the drag coefficient Γ by the relativistic Einstein relation $\Gamma = \kappa/2ET$. Note that the momentum diffusion coefficient κ of heavy quarks can also be converted into another dimensionless form $2\pi TD_s$ in coordinate space using the relation $D_s = 2T^2/\kappa$. Note that, to accurately determine the temperature and momentum dependence of the diffusion coefficient of heavy quarks (κ or D_s), the heavy-ion community has made some elaborate and sgnificant efforts in recent years [107−111]. More detailed reviews can be found in [112, 113]. At each time step, the heavy quarks are boosted into the local rest frame of the expanding medium to update the four-momentum using the Lorentz transformation, boosting them back again to the laboratory frame to update the spatial position. The last correction term $-p_j^g$ corresponds to the momentum recoil of the medium-induced radiated gluon, based on the gluon spectrum calculated by the higher-twist approach [40, 114−116],

$$\frac{\mathrm{d}N}{\mathrm{d}x\mathrm{d}k_\perp^2\mathrm{d}t} = \frac{2\alpha_s C_s P(x)\hat{q}}{\pi k_\perp^4}\sin^2\left(\frac{t-t_i}{2\tau_f}\right)\left(\frac{k_\perp^2}{k_\perp^2 + x^2M^2}\right)^4, \tag{4}$$

where x and $k_\perp$ are the energy fraction and transverse momentum carried by the radiated gluon. C_s is the quadratic Casimir in the color representation, and $P(x)$ the splitting function; $\tau_f = 2Ex(1-x)/(k_\perp^2 + x^2M^2)$ denotes the gluon formation time to take into account the Landau-Pomeranchuk-Migdal (LPM) effects [117, 118]. $\hat{q} = q_0(T/T_0)^3 \cdot p_\mu u^\mu/E$ is the jet transport parameter [119], where T_0 is the highest temperature in the most central A+A collisions, and u^μ the velocity of the medium cell where the heavy quark is located. In considering the fluctuation of medium-induced gluon radiation, we assumed that the number of the radiated gluon during a time step Δt obeys the Possion distribution $f(n) = \lambda^n\mathrm{e}^{-\lambda}/n!$, where the parameter λ denotes the mean number of the radiated gluon which can be calculated by integrating Eq. (4). Once the radiation number n is sampled, the radiated gluon's four-momentum can be further sampled by Eq. (4) one at a time. As discussed above, the momentum update of heavy quarks is driven by Eq. (2). Furthermore, considering the energy loss of the light partons (light quark and gluon) inside the jet cone is essential for the calculation of the full-jet observable. As an effective treatment, the elastic energy loss of light partons is estimated by the perturbative quantum chroodynamics (pQCD) calculations for the hard theral loops (HTL) approximation [120], whereas for the inelastic part, the higher-twist formalism is adopted.

The initial spatial production vertex of jets in nucleus-nucleus collisions is sampled based on the Monte Carlo (MC)-Glauber model [121]. During jet propagation, the velocity and temperature of the expanding QGP medium are provided by the CLVisc hydrodynamic model [122]. In general, the partonic energy loss is assumed to cease at the hadronic phase, namely at the local temperature below $T_c = 0.165$ GeV. In this work, the initial fluctuation of the bulk medium was ignored due to its small influence on the average energy loss of high-p_T jet [123−125]. However, such initial fluctuations of hydrodynamics may be critical for the simultaneous description of the R_{AA} and v_2 of heavy-flavor hadrons at low p_T regions [126, 127]. Notably, based on the isotropic approximation of the QGP medium, κ and $\hat{q}$ of a high-energy heavy quark can be related through a concise expression $\kappa = \hat{q}/2$ [102, 112, 128]. In recent years, the SHELL transport model has been successfully employed to study the medium modifications of both light- and heavy-flavor jet in high-energy nuclear collisions [52, 61−63, 76−80, 129].

IV. RESULTS AND DISCUSSIONS

Note that $\hat{q}$ is the only parameter in our framework that controls the interaction strength for both light and heavy-flavor partons. First, we performed a χ^2 fit of the recent inclusive-jet and b-jet R_{AA} data measured by the ATLAS collaboration [59] to fix the model parameter $\hat{q}$, where the jet R_{AA} is conventionally defined as,

$$R_{AA} = \frac{1}{\langle N_{\mathrm{bin}}^{\mathrm{AA}}\rangle}\frac{\mathrm{d}\sigma^{\mathrm{AA}}/\mathrm{d}y\mathrm{d}p_T}{\mathrm{d}\sigma^{\mathrm{pp}}/\mathrm{d}y\mathrm{d}p_T}. \tag{5}$$

The scaling factor $\langle N_{\mathrm{bin}}^{AA}\rangle$ denotes the number of binary nucleon-nucleon collisions in A+A estimated using the

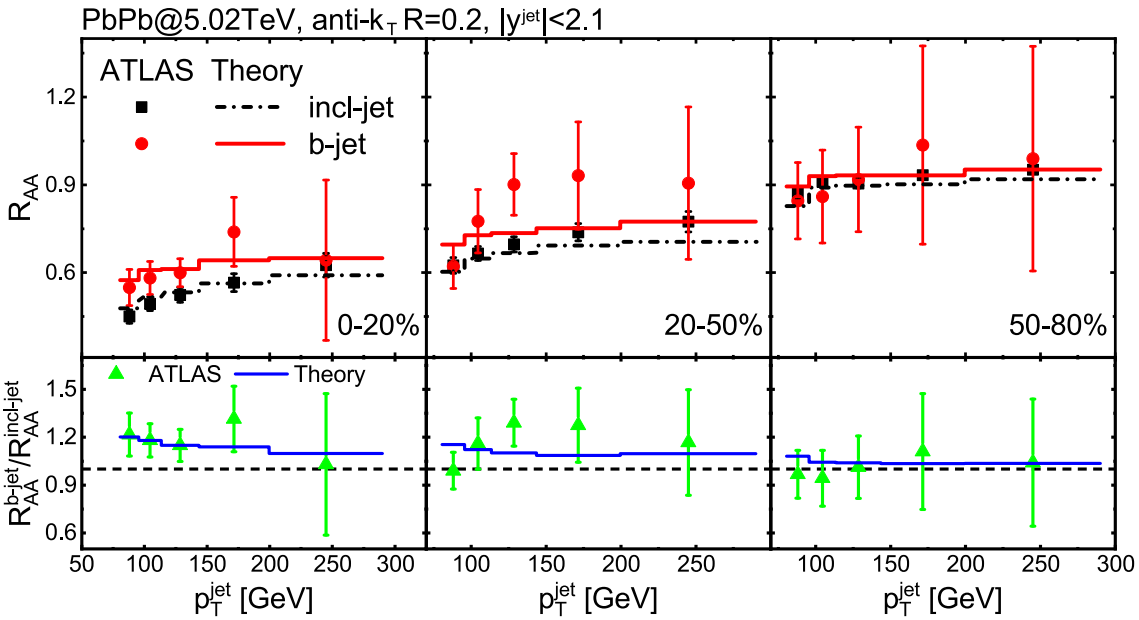

Fig. 6. (color online) The nuclear modification factor R_{AA} of b-jet and inclusive jet in 0%−20%, 20%−50% and 50%−80% Pb+Pb collisions at $\sqrt{s_{NN}}$ = 5.02 TeV compared with ATLAS data (upper panels), along with their ratio $R_{AA}^{\text{b-jet}}/R_{AA}^{\text{incl-jet}}$ (lower panels).

Glauber model [121]. The χ^2 fit of the ATLAS data [59] obtained the optimal value of q_0 = 0.9 GeV^2/fm with χ^2 = 1.29. Using this configuration, the model calculations of b-jet and inclusive jet R_{AA} are compared with the data in Fig. 6, showing good agreement for both the R_{AA} magnitudes and their ratio $R_{AA}^{\text{b-jet}}/R_{AA}^{\text{incl-jet}}$ from central to peripheral Pb+Pb collisions at $\sqrt{s_{NN}}$ = 5.02 TeV. The b-jets experence a more moderate yield suppression than the inclusive jet, which may indicate that the b-jet loses less energy in QGP than the light-flavor jet. However, the HQ-initiated jet is not the dominant contribution for c-jet and b-jet samples, as discussed in Sec. II. The mixture of components in HQ jets complicates the understanding of the mass effect of jet energy loss. Shown in Fig. 7is the nuclear modification factor R_{AA} of both c-jet, b-jet, and inclusive jet in central 0−10% Pb+Pb collisions at $\sqrt{s_{NN}}$ = 5.02 TeV for different jet-cone sizes (R = 0.2, 0.4), at $30 < p_T < 260$ GeV. These calculations were performed at the parton level, and HQ jets (c-jet and b-jet) are defined as jets containing at least one heavy quark inside the jet cone with $p_T^Q > 3$ GeV. As the b-jet has the largest R_{AA}, it is surprising that the c-jet has R_{AA} comparable with that of the inclusive jet for R = 0.2. In addition, for larger jet cone R = 0.4, the yield suppression of c-jet was found to be stronger than that of inclusive jet at $p_T >$ 150 GeV. Similar results were also obtained using the linearized patronic transport LIDO model [130].

In Fig. 8, the averaged jet energy loss (Δp_T) of $Q \to Q$-jet and $g \to Q$-jet were estimated by tracking their propagation in 0−10% Pb+Pb collisions at $\sqrt{s_{NN}}$ = 5.02 TeV for c-jet (upper) and b-jet (lower). First, the total c-jet Δp_T is more significant than that of b-jet with the same initial p_T. Second, by comparing the Δp_T of $c \to c$-jet and $b \to b$-jet, Q-jets initiated by the bottom lose less energy than that by charm, which is the direct embodiment of the mass hierarchy of quark energy loss. Finally,

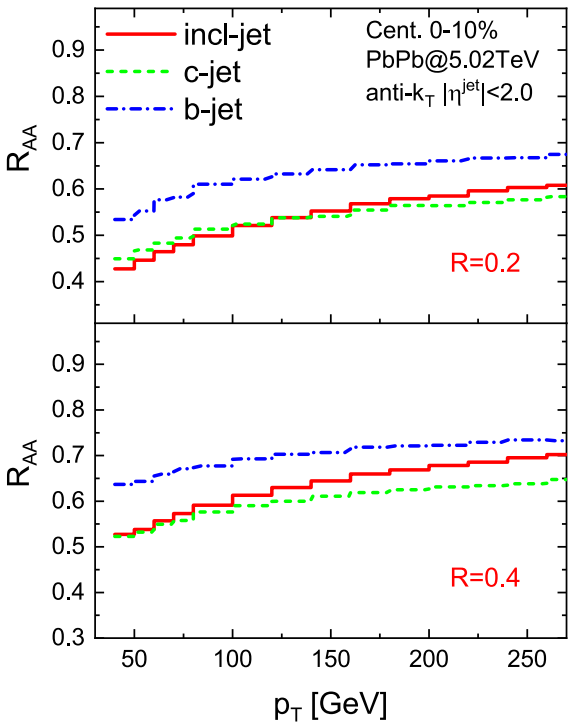

Fig. 7. (color online) The nuclear modification factor R_{AA} of c-jet, b-jet, and inclusive jet in central 0−10% Pb+Pb collisions at $\sqrt{s_{NN}}$ = 5.02 TeV for different jet-cone sizes (R = 0.2, 0.4).

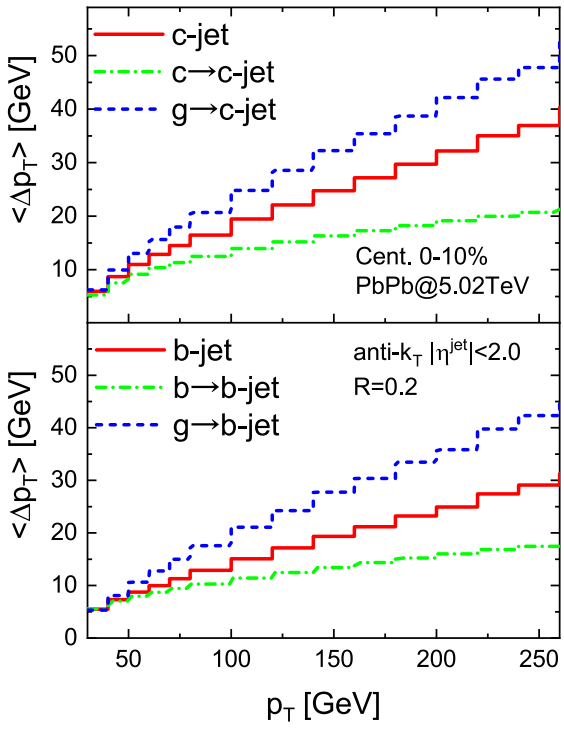

Fig. 8. (color online) The averaged transverse jet energy loss ($\langle\Delta p_T\rangle$) of $Q\to Q$-jet and $g\to Q$-jet in 0−10% Pb+Pb collisions at $\sqrt{s_{NN}}$ = 5.02 TeV, both for c-jet and b-jet.

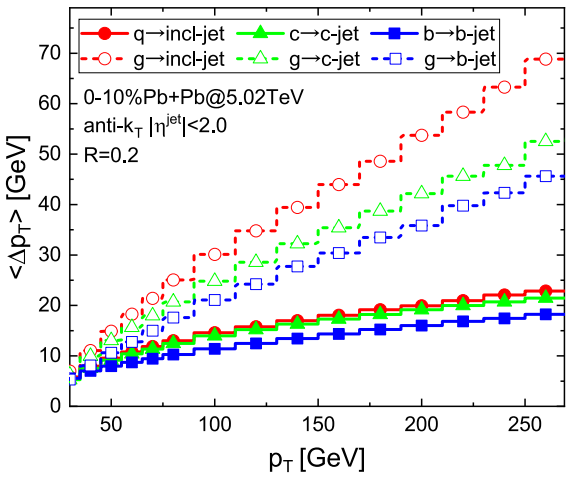

Fig. 9. (color online) The averaged transverse energy loss ($\langle\Delta p_T\rangle$) for the six kinds of jets, $q\to$ incl-jet, $g\to$ incl-jet, $c\to c$-jet, $g\to c$-jet, $b\to b$-jet and $g\to b$-jet, in 0−10% Pb+Pb collisions at $\sqrt{s_{NN}}$ = 5.02 TeV.

we find that $g\to Q$-jet loses much more energy than $Q\to Q$-jet for both c-jet and b-jet. This study employed the p+p events after a full vacuum parton shower as input to simulate the in-medium energy loss. This treatment assumes all heavy quarks were created before the QGP was formed. Hence, the different energy losses of $Q\to Q$-jet and $g\to Q$-jet may only result from their initial features. As presented in Figs. 4 and 5 at the end of Sec. II, the $g\to Q$-jet generally has a more dispersive (z_Q, r_Q) distribution compared to $Q\to Q$-jet, namely plenty of heavy quarks are located in smaller z_Q and larger r_Q regions. Larger r_Q facilitates the dissipation of lost energy from heavy quarks outside the jet cone, which is consistent with the results of the recent measurements of the ATLAS, ALICE, and CMS collaborations [131−136], indicating that the more dispersive the jet structure is, the more energy is lost in the QGP. Moreover, the jets produced by $g\to Q\bar{Q}$ processes usually contain two heavy quarks inside the jet cone, and energy dissipation in the QGP is more efficient compared to the $Q\to Q$-jet.

An overall comparison of the $\langle\Delta p_T\rangle$ for the six kinds of jets ($q\to$ incl-jet, $g\to$ incl-jet, $c\to c$-jet, $g\to c$-jet, $b\to b$-jet and $g\to b$-jet) in 0−10% Pb+Pb collisions at $\sqrt{s_{NN}}$ = 5.02 TeV is shown in Fig. 9, to compare the flavor dependence of jet energy loss intuitively and systematically. First, it is essential that the energy loss of the jet initiated by the parton with different flavors be compared. Excluding the contribution from gluon splitting processes, we find that the jet energy loss obeys the order $\Delta E_{g\to\text{incl-jet}} > \Delta E_{q\to\text{incl-jet}} \gtrsim \Delta E_{c\to c\text{-jet}} > \Delta E_{b\to b\text{-jet}}$, in line with the flavor-dependent parton energy loss expectation. The $b\to b$-jet shows a noticeable mass effect of energy loss compared to the $q\to$incl-jet, whereas the $c\to c$-jet behaves more like a light quark jet at $p_T > 50$ GeV. Comparing the energy loss of $g\to$incl-jet with that of $g\to Q$-jet is also interesting. They are all initiated by the high-energy gluon; however, the latter traverses the QGP as a $Q\bar{Q}$ pair inside the jet. The energy loss of $g\to c$-jet is smaller than that of $g\to$ jet but visibly larger than that of the $q\to$ incl-jet, which indicates that the HQ jets from the gluon splitting lose more energy in the QGP than the light-quark jets. Therefore, the significant contribution of $g\to Q$-jet may be the critical point for understanding the similar R_{AA} of c-jet and inclusive jet shown in Fig. 7. In other words, due to the large fraction of $g\to c$-jet components, the averaged energy loss of c-jet is comparable to that of the inclusive jet. Fig. 10 displays the fractions of $Q\to Q$-jet and $g\to Q$-jet for c-jet (left panel) and b-jet (middle panel) versus jet p_T (left panel) with R = 0.2 and R = 0.4. The fractions of $g\to Q$-jet increase as R varies from 0.2 to 0.4, and accordingly, that of $Q\to Q$-jet decreases for both c-jet and b-jet. For larger jet cones, the enhanced fraction of $Q\to Q$-jet increases the average energy loss of HQ jets. The fractions of quark- and gluon-jet in the inclusive jet sample are shown in the right panel, and they are observed to be insensitive to the jet-cone size. This can explain why the c-jet R_{AA} is smaller than that of the inclusive jet for R = 0.4, as shown in Fig. 7.

So far, we have discussed the jet energy loss of c-jet, b-jet, and inclusive jet by systematically analyzing their component features and fraction variations. Notably, the energy loss of $g\to Q$-jet is significantly more pronounced than that of the $Q\to Q$-jet in nucleus-nucleus

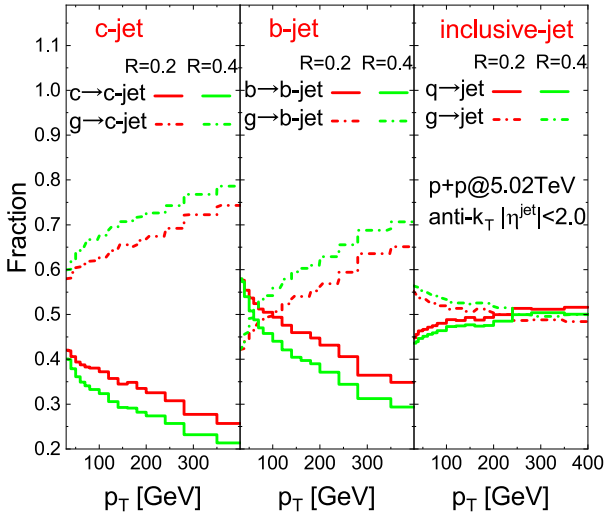

Fig. 10. (color online) The fractional contributions of $c \to c$-jet and $g \to c$-jet to the total c-jet; $b \to b$-jet and $g \to b$-jet to the total b-jet; $q \to$ incl-jet and $g \to$ incl-jet to the inclusive jet; differential cross section versus p_T in p+p collisions at $\sqrt{s}$ = 5.02 TeV, as jet-cone size varies from 0.2 to 0.4.

collisions. Our calculations indicate that $g \to Q$-jet behaves like a gluon-jet but not a heavy quark jet. More efforts in future experimental measurements on $g \to Q$-jet and $Q \to Q$-jet can be helpful in addressing the flavor/mass dependence of jet energy loss. However, these measurements assume that the reconstructed Q-jets from different channels ($Q \to Q$-jet and $g \to Q$-jet) can be identified effectively in the experiment. For this reason, we present the selection methods for separating the two processes $g \to Q$-jet and $Q \to Q$-jet and also estimate the purity of the jet sample selected by these strategies.

As mentioned in Sec. II, the $Q\bar{Q}$ pairs produced by $g \to Q$-jet usually have a narrow opening angle, whereas the one from hard scattering is usually "back-to-back" in the azimuthal plane. We designed the following strategies to select the high-purity sample of $g \to Q$-jet and $Q \to Q$-jet, respectively.

- **Strategy-1** for $g \to Q$-jet: Selecting jets containing two heavy quarks inside the jet-cone. The heavy quark should have $p_T^Q > 2$ GeV.
- **Strategy-2** for $Q \to Q$-jet: Selecting jets containing only one heavy quark inside the jet-cone. Moreover, the selected candidates should have a recoiled HQ jet partner with $p_T > 10$ GeV, and their angle of separation in azimuth plane should satisfy $\Delta\phi_{12} > 2/3\pi$.

To test the performance of the selection strategies, in Fig. 11 we show the purities of the selected $g \to Q$-jet and $Q \to Q$-jet samples in p+p collisions at $\sqrt{s_{NN}}$ = 5.02 TeV for both c-jet and b-jet, where purity is defined as the fraction of the target process in the total selected jet sample,

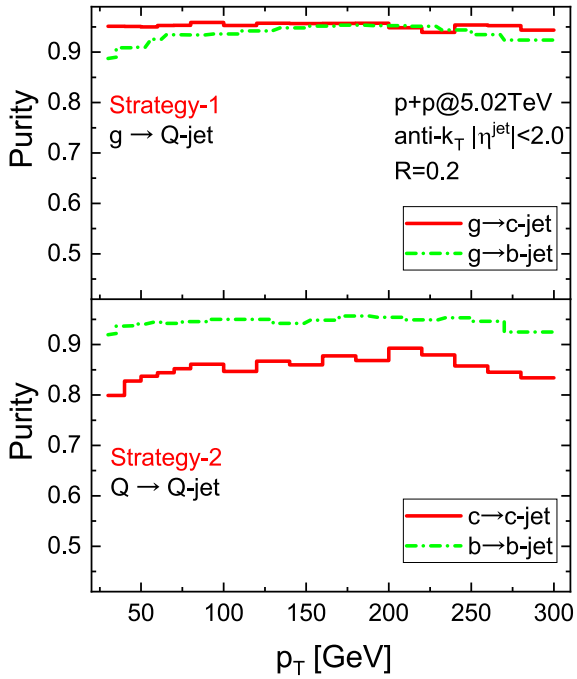

Fig. 11. (color online) Purities of the selected $g \to Q$-jet and $Q \to Q$-jet samples for c-jet and b-jet in p+p collisions at $\sqrt{s_{NN}}$ = 5.02 TeV.

$$\text{Purity} = \frac{\mathrm{d}\sigma/\mathrm{d}p_T[\text{target process}]}{\mathrm{d}\sigma/\mathrm{d}p_T[\text{selected jet sample}]}. \tag{6}$$

In the upper panel of Fig. 11, the purity of the selected $g \to Q$-jet sample is above 0.9 for both c-jet and b-jet. In the lower panel, the purity of the selected $Q \to Q$-jet sample is above 0.8 for c-jet and 0.9 for b-jet. The selection strategies tested in A+A collisions also show similar satisfactory performance.

After establishing the effective strategies for selecting the $g \to Q$-jet and $Q \to Q$-jet, we can directly compare their yield suppression in A+A collisions with the inclusive jet. Although isolating the gluon jet and quark jet in the experiment is difficult, the comparison between $g \to Q$-jet, $Q \to Q$-jet, and inclusive jet may provide a unique opportunity for capturing the flavor/mass dependence of jet quenching, which can be used to test the experiments. Fig. 12 compares the calculatedR_{AA} of selected $c \to c$-jet, $g \to c$-jet, $b \to b$-jet and $g \to b$-jet with that of inclusive jet in 0−10% Pb+Pb collisions at $\sqrt{s_{NN}}$ = 5.02 TeV. Note that $c \to c$-jet, $g \to c$-jet, $b \to b$-jet, and $g \to b$-jet denote the selected samples with the above mentioned strategies. Clearly, the jets initiated by heavy quarks obey the order $R_{AA}^{\text{b-jet}} > R_{AA}^{\text{c-jet}} > R_{AA}^{\text{incl-jet}}$. Namely, by effectively isolating the $Q \to Q$-jet processes, the mass hierarchy of energy loss at jet level ($\Delta E_{\text{incl-jet}} > \Delta E_{\text{c-jet}} > \Delta E_{\text{b-jet}}$) is predicted in nucleus-nucleus collisions. We observe that the yield suppression of $g \to c$-jet is much stronger than that of inclusive jet. As for the

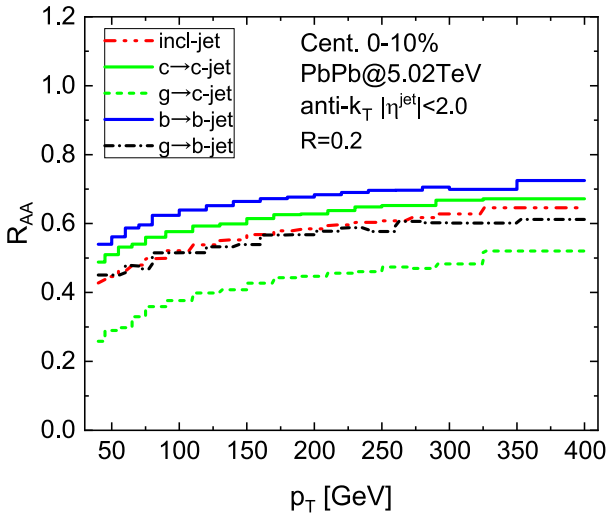

Fig. 12. (color online) R_{AA} of the selected $c \to c$-jet, $g \to c$-jet, $b \to b$-jet, and $g \to b$-jet compared to that of the inclusive jet in 0−10% Pb+Pb collisions at $\sqrt{s_{NN}}$ = 5.02 TeV.

$g \to b$-jet, its yield suppression is obviously stronger than that of $b \to b$-jet and $c \to c$-jet. At high p_T, R_{AA} of $g \to b$-jet is slightly lower than that of inclusive jet whereas their values are close at lower p_T. This may result from the dispersive structure of the b-jets generated by the $g \to b$-jet process, which can lead to more energy loss in the QGP compared to the $b \to b$-jet, similar to the case of the c-jet.

Unlike the treatment in [50], which considers the fragmentation function of high-energy gluon into the heavy-flavor hadron in the hadronization process, in this study, the vacuum splitting of $g \to Q$-jet was simulated before the formation of the QGP medium. The results obtained from different treatments are consistent, indicating that the heavy flavors from gluon splitting suffer a stronger quenching effect than those from the hard scattering in heavy-ion collisions. We next plan to investigate the influence of considering the concrete $g \to Q$-jet splitting time in the QGP medium on the energy loss and substructure modifications of HQ jets, and some recent exploratory studies in this direction are expected to be helpful [137−139]. Moreover, the recent studies have extracted the gluon energy loss by J/Ψ production in Pb+Pb collisions [51] because over 80% J/Ψ is mainly produced by the gluon fragmentation at high p_T. From this point of view, measurement on the $g \to c$-jet production in A+A collisions can similarly build a bridge for understanding the energy loss of the gluon jet.

V. SUMMARY

This paper systematically studies the yield suppression of HQ jets in nucleus-nucleus collisions relative to the p+p, focusing on the energy loss of HQ jets produced by different production mechanisms. The Monte Carlo event generator SHERPA was used to generate the p+p baseline, which matches the NLO hard QCD processes with the resummation of the parton shower. The in-medium evolution of the HQ jets was described by the SHELL transport model, which considers the elastic and inelastic energy loss. The $g \to Q$-jet process significantly contributed to the HQ jet production at high p_T and showed more dispersive structures compared to the $Q \to Q$-jet in p+p collisions. In Pb+Pb collisions at $\sqrt{s_{NN}}$ = 5.02 TeV, our calculations provide descriptions of the inclusive jet and b-jet R_{AA} as measured by the ATLAS collaboration, which remarkably point to the mass effect of jet energy loss. Due to its dispersive substructure, $g \to Q$-jet lost more energy than the $Q \to Q$-jet in the same collision system. Furthermore, because of the dominant contribution of the $g \to c$-jet, the R_{AA} of c-jet was comparable or even smaller than that of inclusive jet. We proposed event selection strategies based on their topological features and tested their performances, which allowed us to distinguish the two processes $g \to Q$-jet and $Q \to Q$-jet according to the final-state jet particle information. By isolating the $c \to c$-jet, $b \to b$-jet, and the jets initiated by heavy quarks, we predicted that the order of their R_{AA} aligns with the mass hierarchy of energy loss. Measurements on the R_{AA} of $Q \to Q$-jet and $g \to Q$-jet in heavy-ion collisions provide a unique opportunity for testing the flavor/mass dependence of energy loss at the jet level.

References

[1] M. Gyulassy, I. Vitev, X. N. Wang *et al.*, In *Quark Gluon Plasma*, edited by Hwa R.C *et al.* (Singapore: World Scientific, 2010), p.123-191
[2] M. Gyulassy and M. Plumer, Phys. Lett. B **243**, 432 (1990)
[3] G. Y. Qin and X. N. Wang, Int. J. Mod. Phys. E **24**(11), 1530014 (2015)
[4] I. Vitev, S. Wicks and B. W. Zhang, JHEP **2008**, 093 (2008)
[5] N. Armesto, N. Borghini, S. Jeon *et al.*, J. Phys. G **35**, 054001 (2008), arXiv: 0711.0974[hep-ph]
[6] I. Vitev and B. W. Zhang, Phys. Rev. Lett. **104**, 132001 (2010)
[7] J. Casalderrey-Solana, D. C. Gulhan, J. G. Milhano *et al.*, JHEP **2014**, 019 (2014)
[8] M. Gyulassy and X. N. Wang, Nucl. Phys. B **420**, 583 (1994), arXiv: nucl-th/9306003[nucl-th]
[9] X. N. Wang and X. F. Guo, Nucl. Phys. A **696**, 788 (2001), arXiv: hep-ph/0102230[hep-ph]
[10] I. Vitev and B. W. Zhang, Phys. Lett. B **669**, 337 (2008), arXiv: 0804.3805[hep-ph]
[11] Y. He, L. G. Pang and X. N. Wang, Phys. Rev. Lett. **125**(12), 122301 (2020), arXiv: 2001.08273[hep-ph]
[12] S. Y. Chen, J. Yan, W. Dai *et al.*, Chin. Phys. C **46**(10), 104102 (2022), arXiv: 2204.01211[hep-ph]

[13] W. Zhao, W. Ke, W. Chen *et al*., Phys. Rev. Lett. **128**(2), 022302 (2022), arXiv: 2103.14657[hep-ph]
[14] Z. Yang, Y. He, I. Moult *et al*., Phys. Rev. Lett. **132**, 011901 (2024), arXiv: 2310.01500[hep-ph]
[15] A. Kumar *et al*. (JETSCAPE), Phys. Rev. C **107**(3), 034911 (2023), arXiv: 2204.01163[hep-ph]
[16] T. Luo, Y. He, S. Cao *et al*., Phys. Rev. C **109**(3), 034919 (2024), arXiv: 2306.13742[nucl-th]
[17] M. Xie, Q. F. Han, E. K. Wang *et al*., Nucl. Sci. Tech. **35**(7), 125 (2024)
[18] H. X. Zhang, Y. X. Xiao, J. W. Kang *et al*., Nucl. Sci. Tech. **33**(11), 150 (2022), arXiv: 2102.11792[hep-ph]
[19] J. W. Kang, S. Wang, L. Wang *et al*., arXiv: 2312.15518
[20] J. W. Kang, L. Wang, W. Dai *et al*., arXiv: 2304.04649
[21] S. Y. Chen, K. M. Shen, X. F. Xue *et al*., arXiv: 2409.13996
[22] M. Connors, C. Nattrass, R. Reed *et al*., Rev. Mod. Phys. **90**, 025005 (2018), arXiv: 1705.01974[nucl-ex]
[23] H. A. Andrews, D. d'Enterria, L. Apolinario *et al*., J. Phys. G **47**(6), 065102 (2020), arXiv: 1808.03689[hep-ph]
[24] L. Cunqueiro and A. M. Sickles, Prog. Part. Nucl. Phys. **124**, 103940 (2022), arXiv: 2110.14490[nucl-ex]
[25] X. Dong and V. Greco, Prog. Part. Nucl. Phys. **104**, 97 (2019)
[26] A. Andronic *et al*., Eur. Phys. J. C **76**(3), 107 (2016)
[27] X. Dong, Y. J. Lee and R. Rapp, Ann. Rev. Nucl. Part. Sci. **69**, 417 (2019), arXiv: 1903.07709[nucl-ex]
[28] J. Zhao, K. Zhou, S. Chen and P. Zhuang, Prog. Part. Nucl. Phys. **114**, 103801 (2020), arXiv: 2005.08277[nucl-th]
[29] B. Chen, M. Yang, G. Chen *et al*., Phys. Rev. C **109**(6), 064909 (2024), arXiv: 2309.02987[nucl-th]
[30] Z. F. Jiang, S. Cao, W. J. Xing *et al*., Phys. Rev. C **105**(5), 054907 (2022), arXiv: 2202.13555[nucl-th]
[31] L. Adamczyk *et al*. (STAR Collaboration), Phys. Rev. Lett. **113**(14), 142301 (2014)
[32] J. Adam *et al*. (ALICE Collaboration), JHEP **2016**, 081 (2016)
[33] A. M. Sirunyan *et al*. (CMS Collaboration), Phys. Lett. B **782**, 474 (2018), arXiv: 1708.04962[nucl-ex]
[34] S. Acharya *et al*. (ALICE Collaboration), JHEP **2018**, 174 (2018), arXiv: 1804.09083[nucl-ex]
[35] B. B. Abelev *et al*. (ALICE Collaboration), Phys. Rev. C **90**(3), 034904 (2014), arXiv: 1405.2001[nucl-ex]
[36] L. Adamczyk *et al*. (STAR Collaboration), Phys. Rev. Lett. **118**(21), 212301 (2017), arXiv: 1701.06060[nucl-ex]
[37] S. Acharya *et al*. (ALICE Collaboration), Phys. Rev. Lett. **120**(10), 102301 (2018), arXiv: 1707.01005[nucl-ex]
[38] A. M. Sirunyan *et al*. (CMS Collaboration), Phys. Rev. Lett. **120**(20), 202301 (2018), arXiv: 1708.03497[nucl-ex]
[39] Y. L. Dokshitzer and D. E. Kharzeev, Phys. Lett. B **519**, 199 (2001), arXiv: hep-ph/0106202[hep-ph]
[40] B. W. Zhang, E. Wang and X. N. Wang, Phys. Rev. Lett. **93**, 072301 (2004)
[41] N. Armesto, C. A. Salgado and U. A. Wiedemann, Phys. Rev. D **69**, 114003 (2004), arXiv: hep-ph/0312106[hep-ph]
[42] M. Djordjevic and M. Gyulassy, Phys. Lett. B **560**, 37 (2003), arXiv: nucl-th/0302069[nucl-th]
[43] J. Adam *et al*. (ALICE Collaboration) , JHEP **2015**, 051 (2015), arXiv: 1504.07151[nucl-ex]
[44] V. Khachatryan *et al*. (CMS Collaboration), Eur. Phys. J. C **77**(4), 252 (2017), arXiv: 1610.00613[nucl-ex]
[45] A. M. Sirunyan *et al*. (CMS Collaboration), Phys. Rev. Lett. **119**(15), 152301 (2017), arXiv: 1705.04727[hep-ex]
[46] M. Aaboud *et al*. (ATLAS), Eur. Phys. J. C **78**(9), 762 (2018), arXiv: 1805.04077[nucl-ex]
[47] M. S. Abdallah *et al*. (STAR), Eur. Phys. J. C **82**(12), 1150 (2022), arXiv: 2111.14615[nucl-ex]
[48] U. A. Acharya *et al. (*PHENIX)., arXiv: 2203.17058
[49] G. Aad *et al*. (ATLAS), Phys. Lett. B **829**, 137077 (2022), arXiv: 2109.00411[nucl-ex]
[50] W. J. Xing, S. Cao, G. Y. Qin *et al*., Phys. Lett. B **805**, 135424 (2020), arXiv: 1906.00413[hep-ph]
[51] S. L. Zhang, J. Liao, G. Y. Qin *et al*., Sci. Bull. **68**, 2003 (2023), arXiv: 2208.08323[hep-ph]
[52] S. Wang, Y. Li, S. Shen *et al*., arXiv: 2308.14538
[53] R. Aaij *et al*. (LHCb), JINST **10**(06), P06013 (2015), arXiv: 1504.07670[hep-ex]
[54] S. Chatrchyan *et al*. (CMS Collaboration), JINST **8**, P04013 (2013), arXiv: 1211.4462[hep-ex]
[55] J. Huang, Z. B. Kang and I. Vitev, Phys. Lett. B **726**, 251 (2013), arXiv: 1306.0909[hep-ph]
[56] H. T. Li and I. Vitev, JHEP **2019**, 148 (2019), arXiv: 1811.07905[hep-ph]
[57] Z. B. Kang, J. Reiten, I. Vitev *et al*., Phys. Rev. D **99**(3), 034006 (2019), arXiv: 1810.10007[hep-ph]
[58] S. Chatrchyan *et al*. (CMS Collaboration), Phys. Rev. Lett. **113**(13), 132301 (2014), arXiv: 1312.4198[nucl-ex]
[59] G. Aad *et al*. (ATLAS), Eur. Phys. J. C **83**(5), 438 (2023), arXiv: 2204.13530[nucl-ex]
[60] A. M. Sirunyan *et al*. (CMS Collaboration), JHEP **2018**, 181 (2018), arXiv: 1802.00707[hep-ex]
[61] W. Dai, S. Wang, S. L. Zhang *et al*., Chin. Phys. C **44**(10), 104105 (2020), arXiv: 1806.06332[nucl-th]
[62] Y. Li, S. Shen, S. Wang and B. W. Zhang, Nucl. Sci. Tech. **35**(7), 113 (2024), arXiv: 2401.01706[hep-ph]
[63] Y. Li, S. Y. Chen, W. Kong *et al*., arXiv: 2409.12742
[64] A. M. Sirunyan *et al*. (CMS Collaboration), Phys. Rev. Lett. **125**(10), 102001 (2020), arXiv: 1911.01461[hep-ex]
[65] S. Acharya *et al*. (ALICE), Nature **605**(7910), 440 (2022), arXiv: 2106.05713[nucl-ex]
[66] G. Aad *et al*. (ATLAS), JHEP **2021**, 131 (2021), arXiv: 2108.11650[hep-ex]
[67] S. Acharya *et al*. (ALICE), JHEP **2019**, 133 (2019), arXiv: 1905.02510[nucl-ex]
[68] R. Vertesi *et al*. (ALICE), Phys. Part. Nucl. **54**(4), 670 (2023), arXiv: 2110.11606[nucl-ex]
[69] A. M. Sirunyan *et al*. (CMS), JHEP **2021**, 054 (2021), arXiv: 2005.14219[hep-ex]
[70] S. Acharya *et al*. (ALICE), Phys. Rev. Lett. **131**(19), 192301 (2023), arXiv: 2208.04857[nucl-ex]
[71] M. Aaboud *et al*. (ATLAS), Phys. Rev. D **99**(5), 052004 (2019), arXiv: 1812.09283[hep-ex]
[72] D. Goncalves, F. Krauss and R. Linten, Phys. Rev. D **93**(5), 053013 (2016), arXiv: 1512.05265[hep-ph]
[73] P. Ilten, N. L. Rodd, J. Thaler and M. Williams, Phys. Rev. D **96**(5), 054019 (2017), arXiv: 1702.02947[hep-ph]
[74] H. T. Li and I. Vitev, Phys. Lett. B **793**, 259 (2019), arXiv: 1801.00008[hep-ph]
[75] H. T. Li, Z. L. Liu and I. Vitev, Phys. Lett. B **827**, 137007 (2022), arXiv: 2108.07809[hep-ph]
[76] S. Wang, W. Dai, B. W. Zhang *et al*., Eur. Phys. J. C **79**(9), 789 (2019), arXiv: 1906.01499[nucl-th]
[77] S. Wang, W. Dai, B. W. Zhang *et al*., Chin. Phys. C **45**(6), 064105 (2021), arXiv: 2012.13935[nucl-th]
[78] Y. Li, S. Wang and B. W. Zhang, Phys. Rev. C **108**(2), 2

(2023), arXiv: 2209.00548[hep-ph]
[79] S. Wang, W. Dai, E. Wang *et al*., Symmetry **15**(3), 727 (2023), arXiv: 2303.14660[nucl-th]
[80] S. Wang, J. W. Kang, W. Dai *et al*., Eur. Phys. J. A **58**(7), 135 (2022), arXiv: 2107.12000[nucl-th]
[81] M. Attems, J. Brewer, G. M. Innocenti *et al*., Phys. Rev. Lett. **132**(21), 212301 (2024), arXiv: 2209.13600[hep-ph]
[82] E. Norrbin and T. Sjostrand, Eur. Phys. J. C **17**, 137 (2000), arXiv: hep-ph/0005110[hep-ph]
[83] A. Banfi, G. P. Salam and G. Zanderighi, JHEP **2007**, 026 (2007), arXiv: 0704.2999[hep-ph]
[84] P. Nason, S. Dawson and R. K. Ellis, Nucl. Phys. B **303**, 607 (1988)
[85] P. Nason, S. Dawson and R. K. Ellis, Nucl. Phys. B **327**, 49 (1989)
[86] W. Beenakker, W. L. van Neerven, R. Meng *et al*., Nucl. Phys. B **351**, 507 (1991)
[87] M. A. G. Aivazis, F. I. Olness and W. K. Tung, Phys. Rev. D **50**, 3085 (1994), arXiv: hep-ph/9312318[hep-ph]
[88] B. A. Kniehl, G. Kramer, I. Schienbein *et al*., Eur. Phys. J. C **41**, 199 (2005), arXiv: hep-ph/0502194[hep-ph]
[89] M. Cacciari, M. Greco and P. Nason, JHEP **05**, 007 (1998), arXiv: hep-ph/9803400[hep-ph]
[90] T. Gleisberg, S. Hoeche, F. Krauss *et al*., JHEP **2009**, 007 (2009), arXiv: 0811.4622[hep-ph]
[91] E. Bothmann *et al*. [Sherpa], SciPost Phys. **7**(3), 034 (2019), arXiv: 1905.09127[hep-ph]
[92] S. Schumann and F. Krauss, JHEP **2008**, 038 (2008), arXiv: 0709.1027[hep-ph]
[93] S. Frixione and B. R. Webber, JHEP **2002**, 029 (2002), arXiv: hep-ph/0204244
[94] R. D. Ball *et al*. (NNPDF), Nucl. Phys. B **809**, 1 (2009), arXiv: 0808.1231[hep-ph]
[95] S. Acharya *et al*. (ALICE), JHEP **2023**, 133 (2023), arXiv: 2204.10167[nucl-ex]
[96] M. Cacciari, G. P. Salam and G. Soyez, Eur. Phys. J. C **72**, 1896 (2012), arXiv: 1111.6097[hep-ph]
[97] M. Cacciari, G. P. Salam and G. Soyez, JHEP **2008**, 063 (2008), arXiv: 0802.1189[hep-ph]
[98] S. Acharya *et al*. (ALICE), JHEP **2022**, 178 (2022), arXiv: 2110.06104[nucl-ex]
[99] G. D. Moore and D. Teaney, Phys. Rev. C **71**, 064904 (2005), arXiv: hep-ph/0412346[hep-ph]
[100] R. Rapp and H. van Hees, arXiv: 0903.1096
[101] M. He, H. van Hees, P. B. Gossiaux *et al*., Phys. Rev. E **88**, 032138 (2013), arXiv: 1305.1425[nucl-th]
[102] S. Cao, G. Y. Qin and S. A. Bass, Phys. Rev. C **88**, 044907 (2013), arXiv: 1308.0617[nucl-th]
[103] R. Katz, C. A. G. Prado, J. Noronha-Hostler *et al*., Phys. Rev. C **102**(2), 024906 (2020), arXiv: 1906.10768[nucl-th]
[104] S. Li, W. Xiong and R. Wan, Eur. Phys. J. C **80**(12), 1113 (2020), arXiv: 2012.02489[hep-ph]
[105] A. Beraudo, A. De Pace, W. M. Alberico *et al*., Nucl. Phys. A **831**, 59 (2009), arXiv: 0902.0741[hep-ph]
[106] K. Ito, Mem. Am. Math. Soc. **4**, 51 (1951)
[107] Y. Xu, S. A. Bass, P. Moreau *et al*., Phys. Rev. C **99**(1), 014902 (2019), arXiv: 1809.10734[nucl-th]
[108] S. Cao, T. Luo, G. Y. Qin and X. N. Wang, Phys. Lett. B **777**, 255 (2018), arXiv: 1703.00822[nucl-th]
[109] A. Francis, O. Kaczmarek, M. Laine *et al*., Phys. Rev. D **92**(11), 116003 (2015), arXiv: 1508.04543[hep-lat]
[110] H. T. Ding, A. Francis, O. Kaczmarek *et al*., Phys. Rev. D **86**, 014509 (2012), arXiv: 1204.4945[hep-lat]
[111] L. Altenkort *et al*. (HotQCD), Phys. Rev. Lett. **132**(5), 051902 (2024), arXiv: 2311.01525[hep-lat]
[112] R. Rapp, P. B. Gossiaux, A. Andronic, R. Averbeck, S. Masciocchi, A. Beraudo, E. Bratkovskaya, P. Braun-Munzinger, S. Cao and A. Dainese, *et al*., Nucl. Phys. A **979**, 21 (2018), arXiv: 1803.03824[nucl-th]
[113] L. Apolinário, Y. J. Lee and M. Winn, Prog. Part. Nucl. Phys. **127**, 103990 (2022), arXiv: 2203.16352[hep-ph]
[114] X. F. Guo and X. N. Wang, Phys. Rev. Lett. **85**, 3591 (2000), arXiv: hep-ph/0005044
[115] B. W. Zhang and X. N. Wang, Nucl. Phys. A **720**, 429 (2003)
[116] A. Majumder, Phys. Rev. D **85**, 014023 (2012)
[117] X. N. Wang, M. Gyulassy and M. Plumer, Phys. Rev. D **51**, 3436 (1995), arXiv: hep-ph/9408344[hep-ph]
[118] B. G. Zakharov, JETP Lett. **63**, 952 (1996), arXiv: hep-ph/9607440[hep-ph]
[119] X. F. Chen, C. Greiner, E. Wang *et al*., Phys. Rev. C **81**, 064908 (2010), arXiv: 1002.1165[nucl-th]
[120] R. B. Neufeld, Phys. Rev. D **83**, 065012 (2011), arXiv: 1011.4979[hep-ph]
[121] M. L. Miller, K. Reygers, S. J. Sanders *et al*., Ann. Rev. Nucl. Part. Sci. **57**, 205 (2007)
[122] L. G. Pang, H. Petersen, Q. Wang *et al*., Phys. Rev. Lett. **117**(19), 192301 (2016), arXiv: 1605.04024[hep-ph]
[123] T. Renk, H. Holopainen, J. Auvinen *et al*., Phys. Rev. C **85**, 044915 (2012), arXiv: 1105.2647[hep-ph]
[124] B. Betz, M. Gyulassy and G. Torrieri, Phys. Rev. C **84**, 024913 (2011), arXiv: 1102.5416[nucl-th]
[125] S. Cao, Y. Huang, G. Y. Qin *et al*., J. Phys. G **42**(12), 125104 (2015), arXiv: 1404.3139[nucl-th]
[126] J. Noronha-Hostler, B. Betz, J. Noronha *et al*., Phys. Rev. Lett. **116**(25), 252301 (2016), arXiv: 1602.03788 [nucl-th]
[127] C. A. G. Prado, J. Noronha-Hostler, R. Katz *et al*., Phys. Rev. C **96**(6), 064903 (2017), arXiv: 1611.02965 [nucl-th]
[128] S. Cao, G. Coci, S. K. Das *et al*., Phys. Rev. C **99**(5), 054907 (2019), arXiv: 1809.07894[nucl-th]
[129] S. Wang, Y. Li, J. W. Kang *et al*., arXiv: 2408.10924
[130] W. Ke, X. N. Wang, W. Fan *et al*., PoS **HardProbes 2020**, 060 (2021), arXiv: 2008.07622[nucl-th]
[131] S. Acharya *et al*. (A Large Ion Collider Experiment and ALICE), Phys. Rev. Lett. **128**(10), 102001 (2022), arXiv: 2107.12984[nucl-ex]
[132] G. Aad *et al*. (ATLAS), Phys. Rev. C **107**(5), 054909 (2023), arXiv: 2211.11470[nucl-ex]
[133] S. Acharya *et al*. (ALICE), JHEP **2018**, 139 (2018), arXiv: 1807.06854[nucl-ex]
[134] S. Acharya *et al*. (ALICE), arXiv: 2303.13347
[135] G. Aad *et al*. (ATLAS), Phys. Rev. Lett. **131**(17), 172301 (2023), arXiv: 2301.05606[nucl-ex]
[136] A. Hayrapetyan *et al*. (CMS), arXiv: 2405.02737
[137] W. Fan *et al*. (JETSCAPE), Phys. Rev. C **107**(5), 054901 (2023), arXiv: 2208.00983[nucl-th]
[138] M. Zhang, Y. He, S. Cao and L. Yi, Chin. Phys. C **47**(2), 024106 (2023), arXiv: 2208.13331[nucl-th]
[139] R. Modarresi-Yazdi, S. Shi, C. Gale *et al*., arXiv: 2407.19966